

Feasibility of supercontinuum sources for use in glucose sensing by absorption spectroscopy

Silje S. Fuglerud^{a,b}, Karolina Milenko^a, Reinold Ellingsen^a,
Astrid Aksnes^a, and Dag R. Hjelme^a

^aDepartment of Electronic Systems, Norwegian University of Science and Technology,
Trondheim NO-7491, Norway

^bSt. Olavs University Hospital, Trondheim NO-7030, Norway

ABSTRACT

Diabetes mellitus 1 requires tight control of the blood glucose levels to avoid harmful effects of either too high (hyperglycemia) or too low (hypoglycemia) blood sugar. Due to the availability of low-cost components, fiber-coupled near infrared (NIR) absorption spectroscopy could be a feasible measurement method. From the molar absorptivity of glucose, it is shown that to achieve high accuracy using near infrared spectroscopy for glucose sensing, relative noise levels should not exceed 0.003%. Two supercontinuum (SC) sources and one broadband lamp were investigated with a low-cost portable spectrometer. The SNR of the two SC sources was limited by amplitude fluctuations and could be improved by averaging. The SNR of the broadband source was found to be largely limited by the detector noise due to the weak intensity. 16 aqueous glucose samples ranging from 0 to 500 mM were measured with the broadband source and an SC laser. A partial least squares regression (PLSR) model was built for both measurement sets, yielding root mean square errors of 49 and 54 mM, illustrating how the limit of detection is restrained by the high relative intensity noise. A reference arm setup was built and could account for much of the variability of the SC source. A glucose measurement series using this setup and five samples (100 to 500 mM) yielded a root mean square error of 10.6 mM. The results indicate that an SC source can be feasible for absorption spectroscopy in a reference arm setup.

Keywords: Near infrared, glucose, supercontinuum laser, fiber sensing.

1. INTRODUCTION

Diabetes mellitus 1 requires precise control of the blood glucose levels to avoid harmful effects of either too high (hyperglycemia) or too low (hypoglycemia) blood sugar. As an alternative to electrochemical sensors, optical glucose sensing could provide a long-term option for continuous glucose measurements.¹ Near infrared (NIR) absorption spectroscopy has promising aspects for optical glucose sensing due to the availability of low-cost components. Research has been done on both non-invasive devices utilizing scattering from the skin and on measuring aqueous glucose from a body fluid. The focus of this work will be on aqueous glucose, as the measurement is less prone to error caused by changes in the physiological state of the user. To reliably treat diabetes patients with physiological glucose concentrations of approximately 2 to 30 mM (non-diabetic range: 4 to 8 mM), an error lower than 1 mM is necessary. Such a low error has been achieved in optical bench-top experiments of aqueous glucose mixtures in laboratories with bulky and expensive equipment.² Lower-cost portable equipment must be adopted for the technology to be available to patients. Herein, we investigate the limiting effects of noise in low-cost, portable NIR detectors and sources, illustrated with a series of glucose measurements.

We look at three white-light sources with vastly different noise characteristics: a stable broad band source and two supercontinuum (SC) sources with considerably higher levels of intensity noise. SC sources have seen an increase in new opportunities with the development of photonic crystal fibers in the late 1990s.³ Enormous interest has been shown for SC in recent years, with applications including optical coherence tomography, optical communication, and super-resolution microscopy.⁴ SC sources boast advantages such as low pulse energies

Further author information and correspondence to S.S.F.: E-mail: silje.fuglerud@ntnu.no

to generate the supercontinuum, high levels of coherence and brightness, low dispersion and ultrabroadband continuum exceeding 1000 nm.⁴ Until now, SC sources have not often been employed for absorption spectroscopy due to increased amplitude noise as compared to incandescent lamps.⁵ Nonetheless, an SC source was recently applied in photoacoustic sensing of glucose.⁶ The SC sources are explored here due to their bright output combined with a broad spectrum generation.

2. THEORY

From Beer-Lambert's law,⁷ the concentration of i analytes in a liquid is related to the transmitted light intensity

$$-\ln\left(\frac{I}{I_0}\right) = \sum_i (\epsilon_i c_i + \mu_i) l, \quad (1)$$

where I and I_0 are the transmitted intensity and the reference intensity, ϵ_i is the molar absorptivity, c_i is the concentration, μ_i is the assumed negligible scattering within the sample and l is the path length. The scattering is often ignored for transmission through liquids. For aqueous solutions with a solute, a reduction in the concentration of water must be accounted for by the displacement factor f such that $\alpha = \epsilon_{\text{sol}} c_{\text{sol}} + \epsilon_{\text{H}_2\text{O}}(c_{\text{H}_2\text{O}} - f c_{\text{sol}})$.

The absorptivity of water⁸ and the molar absorptivity of glucose⁷ are plotted in Fig. 1a), ignoring the highly absorbing water peaks around 2000 nm and 2400 nm. It is of importance to note that the molar absorptivity of glucose is four orders of magnitude lower than that of water. The change in the relative intensity I/I_0 can be found from Eq. 1. For a change in the glucose concentration from 4 mM to 3 mM, the corresponding change in relative intensity is in the range 0.001 % to 0.003 %, as illustrated in Fig. 1b). An *in vivo* glucose sensor must be sensitive in this region, as such a drop in blood glucose values would indicate hypoglycemia and require immediate action. From a noise per pixel consideration for a grating spectrometer with a detector array, an approximate boundary on the relative intensity noise (RIN) ($\text{RIN} = \sigma/I$) of an absorption spectroscopy sensor for use *in vivo* is 0.003 %.

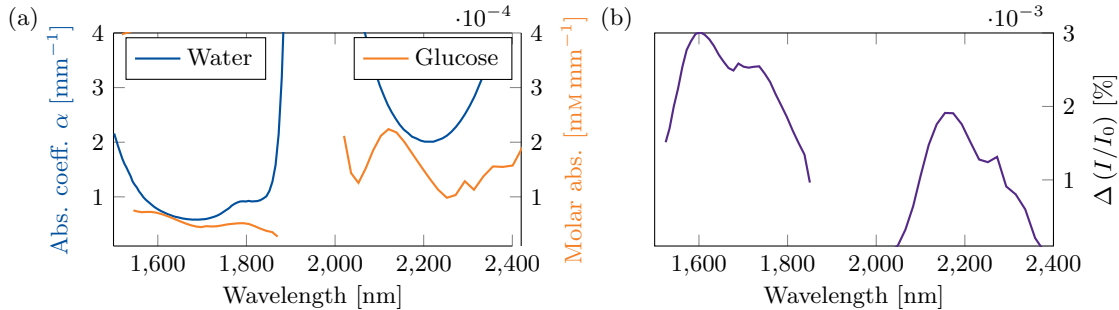


Figure 1: a) Absorptivity of water and molar absorptivity of glucose as tabulated.^{7,8} Note the difference in the orders of magnitude between water and glucose. b) The difference in the intensity of 4 mM and 3 mM for $l = 1$ mm.

First we define the parameters that will be used to characterize and discuss the noise levels in the system. For an acquired spectra of p wavelength channels, the measurement at each channel will have some uncertainty. The variation at a given wavelength is defined as

$$\sigma_\lambda^2 = \frac{1}{n-1} \sum_{i=1}^n (I_{i,\lambda} - \bar{I}_\lambda)^2, \quad (2)$$

where n is the number of data acquisitions with intensity I_i and \bar{I} is the average intensity of the given wavelength.³ It can be shown⁹ that by averaging across several acquired spectra, the standard deviation of each wavelength declines as $\sigma_{\text{avg},\lambda} = \sigma_\lambda/\sqrt{N}$, where N is the number of spectra that are averaged. The average variance across specified wavelength channels will often be used here when the channels display similar characteristics.

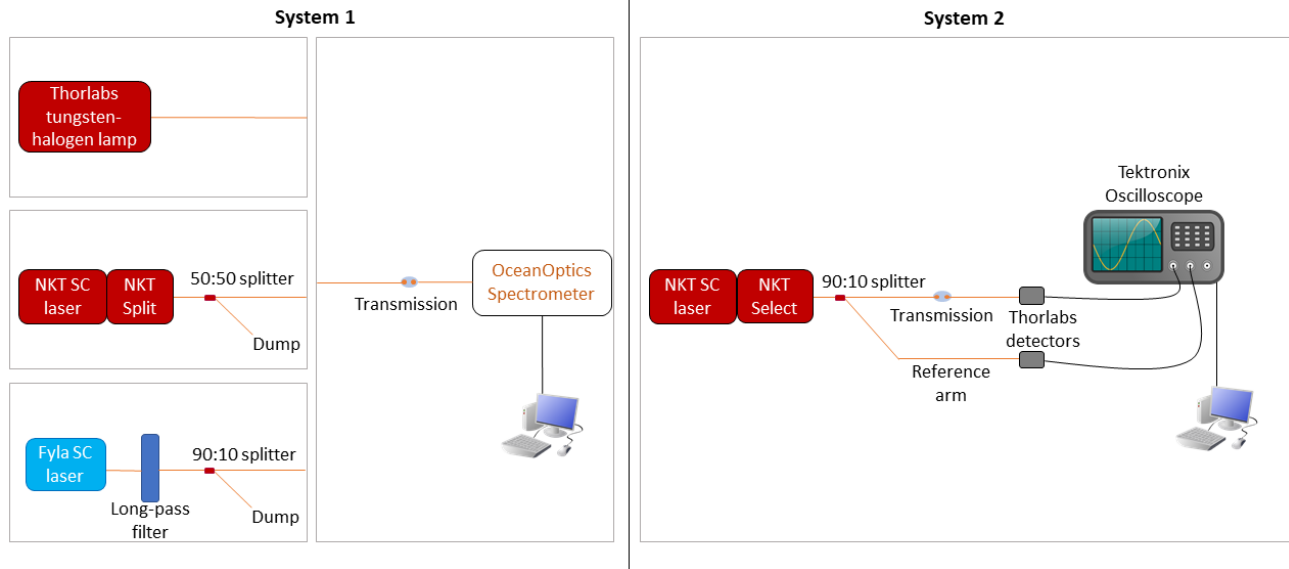


Figure 2: Schematic of the two system setups explored in this work. For the characterization, the sample transmission was bypassed and all of the light was fiber coupled.

To obtain an estimate for the expected variance, we consider a simple case. For a light from a thermal source the photon number obeys the Poisson probability distribution, with a variance $\sigma_n^2 = \bar{n}$, where \bar{n} is the average number of photons counted by the photodetector within a time T , proportional to \bar{I} .¹⁰ Taking into account the effect of N averages, the RIN then simplifies to

$$\text{RIN}_{\text{poiss}} = \frac{\sqrt{\bar{n}/N}}{\bar{n}} = \frac{1}{\sqrt{N\bar{n}}}. \quad (3)$$

We will present two system setups. For the second one, a receiver system consisting of a photodetector and an oscilloscope, the variance can be described by

$$\sigma_{\text{tot}}^2 = \sigma_i^2 + \sigma_T^2 + \sigma_{\text{osc}}^2, \quad (4)$$

where σ_i^2 is the photocurrent variance, σ_T^2 is the thermal noise current variance and σ_{osc}^2 is the noise added by the oscilloscope. The photocurrent variance and thermal noise current variance can be expressed as $\sigma_i^2 = 2e\bar{i}B$ and $\sigma_T^2 = 4kTB/R$, where e is the elementary charge, \bar{i} is the average current, B is the bandwidth, T is the temperature, k is Boltzmann's constant and R is the resistance.¹⁰ Two co-varying channels will be used in the analysis. For a function of two measurable variables $f = A/B$, where the input variables A and B are dependent and have variances σ_A^2, σ_B^2 and covariance σ_{AB}^2 , the final variance will be^{11,12}

$$\frac{\sigma_f^2}{f^2} = \frac{\sigma_A^2}{A^2} + \frac{\sigma_B^2}{B^2} - 2\frac{\sigma_{AB}}{AB}. \quad (5)$$

In the coming sections, the coefficient of variation (CV) will be discussed, which refers to the standard deviation of the variable divided by the magnitude of the variable (e.g. σ_f/f).

3. EXPERIMENTAL COMPARISON

Two system setups are explored, as shown in Fig 2. Setup 1 consists of a light source (broadband lamp or an SC laser) connected to a low-cost spectrometer. Setup 2 is an implementation of a reference arm designed to account for the intensity variance from the SuperK SC laser. The wavelength is chosen by an acousto-optic tunable filter (AOTF) (SuperK Select, NKT Photonics), two arms connected to photo detectors and an oscilloscope for data acquisition.

Table 1: The variation in detected light (averaged over 200 scans) and the measured peak values corresponding to 50 % of the original source power of the SuperK and 10 % of the SCT500. The relative intensity was averaged over wavelengths 1200 to 2200 nm.

Instrument	Tabulated power [mW]	Integration time [ms]	Measured peak brightness [counts/ms]	RIN _{meas} [%]	RIN _{poiss} [%]
SLS201L broadband lamp	10	10	666	0.4023	0.1061
SuperK Compact SC laser	200	1	56 200	0.3503	0.0365
SCT500 SC laser	500	1	46 100	0.1570	0.0403

3.1 Noise characterization

System 1

An OceanOptics NIRQuest 512-2.5 spectrometer with a 5 μm slit for high resolution was used to detect the transmitted light. The detector dark signal level per pixel was measured to 100 to 300 counts/ms, with an average measured standard deviation of $\sigma = 0.6$ counts (int. time: 1 ms, avg. 200). Three light sources were investigated by fiber-coupling to the spectrometer; A Thorlabs SLS201L broadband light source, a Fyla SCT500 SC laser (20 MHz repetition rate) and an NKT Photonics SuperK Compact SC laser (1 Hz to 20 kHz repetition rate) with a Split module to remove lower wavelengths of the spectrum. The SCT500 has a strong pump at 1100 nm which was filtered out by a long-pass filter with onset at 1200 nm (Thorlabs). Due to detector saturation, 90 % of the power was dumped with a 90:10 splitter. The SuperK Split module gave a broad output from 1100 nm to 2200 nm. Half of the power was removed with a 50:50 splitter (MM, Thorlabs) to avoid saturation.

The intensities and measured standard deviation noise level averaged over the spectrum are shown in Table 1, along with the full spectra in Fig. 3a). The spectrometer output reads counts for a given integration time (SC: 1 ms; broadband: 10 ms). To not exceed a RIN (σ/\bar{I}) of 0.003 % for the measured $\sigma_{\text{det}} = 0.6$ counts, the source must supply a minimum of 16 700 counts/ms if the system is limited by detector noise. The expected RIN based on Eq. 3 is also tabulated in Table 1 under the assumption that \bar{n} equals 2/3 of the peak brightness. With 200 averages and 10 ms integration time, the expected estimated RIN ≈ 0.11 % for the broad band source, which is slightly higher than the measured value. The measured value could be higher due to some intensity noise from the source. Both from the measurement and estimate of the RIN, it is clear that the power of the broad band source of 666 counts/ms is insufficient. Considering the two SC sources, the estimated RIN based on Poisson statistics is around 0.04 %, which is much lower than what was measured. Based on a pure number count, the SC lasers both display adequate peak brightness. However, the intensity output of non-linear spectrum generation is not stable and adds to the measurement uncertainty. In the best case, the noise in SC sources is shot noise limited, as has been investigated and discussed previously.^{13,14} The signal to noise ratio (SNR) can be improved by averaging until other noise sources become dominant,¹⁴ the effect is shown on the SuperK in Fig. 3b). It is also worth noting that the number of counts needed to exceed the detector noise is considerably higher (about 100 times) if we assume Poisson statistics on the detector (and do not use the dark noise $\sigma_{\text{det}} = 0.6$ counts, but rather Eq. 3). In fact, such a high count number would saturate the detector. The issue might be resolved by considering that the lower limit of error per pixel set may be too strict. The peaks in the NIR range are broad, and neighboring wavelength absorption measurements are not independent. A crude estimate of such a reduction is $\sigma = \sigma_0/\sqrt{p/N_v}$, with p channel variables that are transformed to N_v latent variables. For $p = 512$ and $N_v = 5$, the limit of a RIN of 0.003 % would increase by approximately a tenfold to 0.03 %, which could be achieved with the OceanOptics Spectrometer using a light source with the noise characteristics of the broad band source and the peak brightness of an SC laser.

System 2: Reference arm

The SuperK Compact SC laser was combined with the SuperK Select module (NKT Photonics) which utilizes an AOTF to select wavelengths with bandwidth of 6.4 nm to 19.8 nm for the IR filter used. The tunable range was 1175 nm to 2000 nm. The SuperK Compact was set to a low repetition rate of 231 Hz. The light was split with a 90:10 splitter (MM, Thorlabs), where a sample of pure water was placed in the arm with 90 % of the signal strength. Two InGaAs detectors (DET01CFC, Thorlabs) with range 800 nm to 1700 nm terminated the arms. The detectors were connected to a DPO4032 Oscilloscope (Tektronix). The oscilloscope was used to trigger on

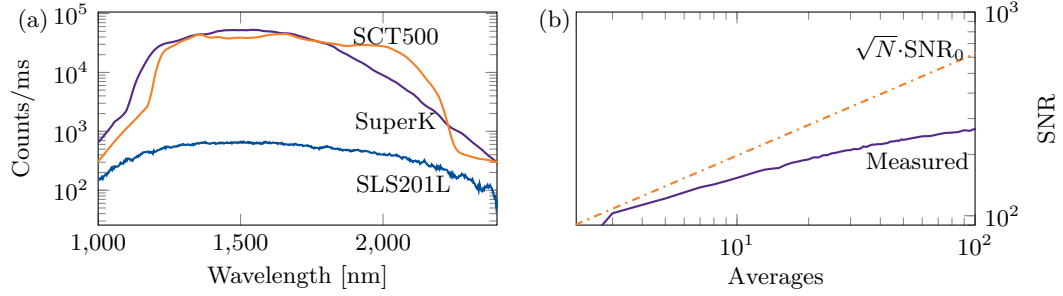


Figure 3: a) The spectra of the three measured sources. b) Increase in SNR averaged over wavelengths 1200 to 2200 nm due to decreased variance from averaging the SuperK spectra. The deviation from $\sqrt{N} \cdot \text{SNR}_0$ indicates contribution from low-frequency noise sources and that the system is not shot noise limited.

Table 2: Standard deviation in the two oscilloscope channels, 50 Ω input. σ_{osc} was measured, the other noise sources were estimated.

Channel/Variance	σ_i [μA]	σ_T [μA]	σ_{osc} [μA]	σ_{tot} [μA]
Channel A (sample)	21	12	41	48
Channel B (ref)	9	12	43	45

the rising edge of an incoming pulse and to transfer the single shot of both channels to the computer. This takes care of high data-rates but also sets a time constraint on the acquisitions. The oscilloscope has a sample rate of 1.25 GHz which is able to resolve the 1.2 GHz output of the detectors. With a pulse width of < 2 ns, fine features of the pulse were not resolved. The waveform was directly transferred to the computer, and the area under the pulse integrating 20 points was found to be the most stable parameter and used in further analysis.

In Fig 4a), the CV of the recorded integrated areas under the curve, that is σ_A/A and σ_B/B in Eq. 5, is shown as a function of wavelength. Here, the light was propagated through water. The sample and reference channels (channels A and B) exhibit relatively high CV, from around 2% up to 6%. The channels are highly correlated as seen by the decrease in CV by performing $f = A/B$. The third trace shows σ_f/f , which is mostly lower than 1%, except for an increase around the strongly absorbing water peak at 1400 nm to 1500 nm which lowered the SNR and a slight increase at the high end of the spectrum, where the detector is not as sensitive. By adding the reference arm, we have been able to decrease the error, which was initially limited by pulse-to-pulse variation, to less than 1%. Until now, we have assumed that the major contribution to the variance was the variation from pulse-to-pulse in the source. However, there are other sources of noise as mentioned in Eq. 4. An analysis was conducted of the lower limit of variance that can be expected for such a system assuming that the reference completely removed the pulse-to-pulse variation. The resulting values are shown in Table 2. The higher variation in Channel 1 is due to the unequal split between the arms and that the sample arm transmits 90% of the emitted power. The oscilloscope dark noise level is also slightly higher with larger input. Inserting $\sigma_{A,\text{tot}}$ and $\sigma_{B,\text{tot}}$ into Eq. 5 and assuming they are not correlated, an approximate lower limit of the standard deviation of the two channels with no intensity noise of 0.46% is obtained. This limit is almost reached for certain wavelengths after we have corrected for the intensity noise. An improvement in this system can be obtained by replacing the oscilloscope with a lower-noise alternative.

In comparison with System 1, the reference arm allowed us to obtain a remarkably stable signal. As mentioned in the Theory section, averaging can be advantageous and can decrease the standard deviation by a factor $1/\sqrt{N}$ for N averages. The increased SNR as a function of averages is presented in Fig. 4b). In comparison with the improvement in SNR with averaging for System 1 (Fig. 3b)), the SNR is almost doubled. This is not just a doubling in performance, as the two graphs are not entirely comparable. The real improvement in performance is more than double. For System 1, the lowest integration time (1 ms) of the oscilloscope and the set frequency of 20 kHz for the SuperK, an averaging of 20 is already in place. For System 2, single pulses have been recorded.

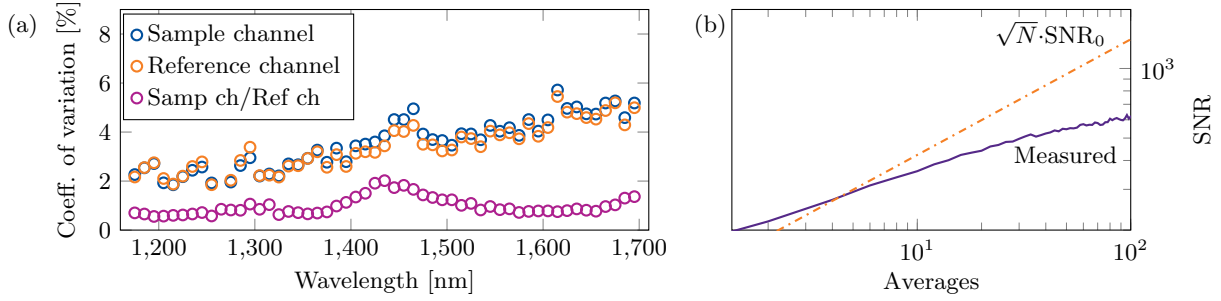


Figure 4: a) The CV on the channels from the spectrum measured with the SuperK in System 2 through water. b) The increase in SNR averaged over wavelengths 1175 nm to 1675 nm.

3.2 Glucose measurements

System 1

To illustrate the effect of the light sources, glucose solutions were measured in transmission mode between multi mode (MM) fibers. A lens with diameter 160 μm was created by an arc (FSM-100P ARCMaster, Fujikura) on the MM fiber tips to decrease losses.^{15,16} The fibers were fixed with two fiber chucks (Newport) and aligned 1 mm apart. D-(+)-Glucose powder (Sigma-Aldrich) was dissolved in pure water, creating 16 concentrations ranging from 0 mM to 500 mM. Supraphysiological concentrations were included to ensure the limit of detection was exceeded. Using the broadband lamp (int. time: 80 ms, avg: 200) and the SuperK SC laser (int. time: 1 ms, avg: 1000), the samples were placed between the fibers and measured at least twice in random order. The sample sets were preprocessed with multiplicative scattering correction (MSC) and a multivariate regression model was built using partial least squares regression (PLSR) on the first derivative. For the broadband source, a model with five latent variables yielded a root mean square error (RMSE) of calibration of 53.8 mM and a RMSE of cross-validation of 65.5 mM. For the SuperK SC laser, a model with four latent variables yielded a RMSE of calibration 48.9 mM and a RMSE of cross-validation of 73.4 mM (Fig. 5). The detector noise for the broad band source and the amplitude noise for the SC source limits the prediction accuracy to a level higher than 50 mM, far above normal physiological glucose levels.

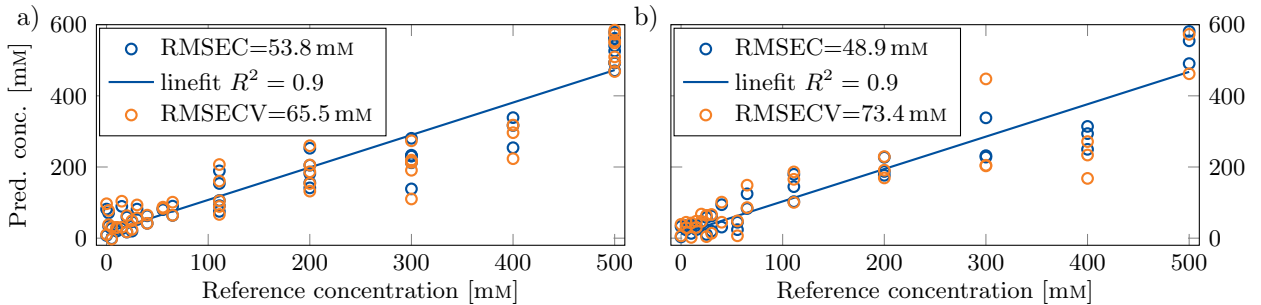


Figure 5: The prediction from a multivariate regression on the spectrum measured with a) SLS201L and b) SuperK.

System 2: Reference arm

A smaller glucose sample set of five samples ranged 0 mM to 500 mM was prepared and measured for System 2. The fiber transmission was set up in the same way as for System 1. The acquisition was made with a pulse frequency of 231 Hz across 53 wavelengths between 1175 nm to 1700 nm, and 100 acquisitions were averaged to obtain the spectra. The sample sets were preprocessed in the same way as the samples from System 1 with MSC and the PLSR model with two latent variables gave an RMSE of 10.6 mM and an RMSE of calibration of 24.9 mM (Fig. 6). Although the sample set was smaller, a large improvement on the error can be observed when utilizing the reference arm as compared to System 1. This can be attributed to the increased SNR. A smaller wavelength

range was included in System 2 (detector constraint), which excluded the vibrations from the combination band (2050 nm to 2300 nm). With the higher wavelengths included, the prediction could have been improved further.

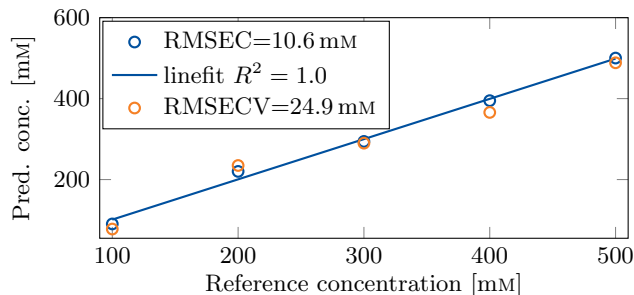


Figure 6: The prediction from a multivariate regression on the spectrum measured with the SuperK in System 2.

4. DISCUSSION AND CONCLUSION

Measurements with the broadband lamp showed low sensitivity due to the insufficient power as compared to the shot noise limited detector noise level of the spectrometer used. The two brighter SC sources investigated fulfill the power requirement but displayed too high variability to be able to detect the weak signal from the glucose molecules as is. The restraint posed by noise on the portable glucose sensing setup sets the current limit of detection to approximately 50 mM using the low-cost spectrometer. A reference arm was shown to adapt the variability of the source and gave a doubling in SNR. With improved electronics and a detector which can also detect wavelengths up to 2300 nm, such a reference arm setup could enable the use of SC sources for spectroscopy measurements of glucose. Although pre-processing methods such as MSC can remove baseline shifts, random changes within the spectrum on a time-scale of minutes is challenging to correct for post-measurement. In order to use SC sources for high-sensitivity measurements we therefore conclude that a pulse-variability reference is essential. This can be achieved with a setup such as System 2, or by adding a second spectrometer, which would considerably increase the cost. Due to the broad peaks in the NIR range, neighboring wavelength absorption measurements are not independent. The lower limit of error per pixel set may therefore be too strict and will be investigated further.

Acknowledgements

We thank Sven Schwermer and Dominik Osinski for their help in programming the data acquisition from the oscilloscope.

Silje S. Fuglerud is funded by the Central Norway Regional Health Authority, project number 46055510. The project is part of the Double Intra-peritoneal Artificial Pancreas project, project number 248872, funded by the Research Council of Norway.

REFERENCES

- [1] I. L. Jernelv, K. Milenko, S. S. Fuglerud, D. R. Hjelme, R. Ellingsen and A. Aksnes, “A review of optical methods for continuous glucose monitoring,” *Appl. Spectrosc. Rev.* (2018), DOI: 10.1080/05704928.2018.1486324.
- [2] M. Goodarzi and W. Saeys, “Selection of the most informative near infrared spectroscopy wavebands for continuous glucose monitoring in human serum,” *Talanta* **146**, 155-165 (2016).
- [3] M. Bondu, “Supercontinuum sources in the practice of multimodal imaging”, PhD Thesis, University of Kent, 2018.
- [4] R. R. Alfano, “The Supercontinuum Laser Source: The Ultimate White Light; 3rd ed.; Preface”, Springer (2016), ISBN 978-1-4939-3326-6.
- [5] C. A. Michaels, T. Masiello, and P. M. Chu, “Fourier Transform Spectrometry with a Near-Infrared Supercontinuum Source”, *Applied Spectroscopy* **63**(5), 538–543 (2009).
- [6] M. J. Dasa, C. Markos, J. Janting, and O. Bang, “Multispectral photoacoustic sensing for accurate glucose monitoring using a supercontinuum laser” *J. Opt. Soc. Am. B.* **36**(2), A61–A65 (2019).

- [7] A. K. Amerov, J. Chen and M. A. Arnold, "Molar Absorptivities of Glucose and other Biological Molecules in Aqueous Solutions over the First Overtone and Combination Regions of the Near-Infrared Spectrum," *Appl. Spectrosc.*, **58**(10), 1195-1204 (2004).
- [8] L. Kou, D. Labrie and P. Chylek, "Refractive indices of water and ice in the 0.65 to 2.5 μm spectral range," *Appl. Opt.* **32**, (1993).
- [9] E. B. Loewenstein, "Reducing the effects of noise in a data acquisition system by averaging", Application note, National Instruments, 2000. <http://users.df.uba.ar/jaliaga/dither/AN152.pdf>.
- [10] B. E. A. Saleh and M. C. Teich, "Fundamentals of Photonics; 2nd ed.; Ch. 18," Wiley, 2007.
- [11] P. Fornasini, "The uncertainty in physical measurements: an introduction to data analysis in the physics laboratory, p. 161-165," Springer (2008), ISBN 978-0-387-78649-0.
- [12] E. F. Meyer, "A Note on Covariance in Propagation of Uncertainty," *J. Chem. Educ* **74**(11), 1339–1340 (1997).
- [13] K. L. Corwin, N. R. Newbury, J. M. Dudley, S. Coen, S. A. Diddams, K. Weber, and R. S. Windeler, "Fundamental Noise Limitations to Supercontinuum Generation in Microstructure Fiber" *Phys. Rev. Lett.* **90**(11), 113904 (2004)
- [14] W. J. Brown, S. Kim, and A. Wax, "Noise characterization of supercontinuum sources for low-coherence interferometry applications," *J. Opt. Soc. Am. A* **31**, 2703–2710 (2014).
- [15] S. S. Fuglerud, K. Milenko, R. Ellingsen, A. Aksnes, D. R. Hjelme, "Glucose sensing by absorption spectroscopy using lensed optical fibers," *Appl. Opt.* **58**(10), 2456–2462 (2019).
- [16] K. Bescherer, D. Munzke, O. Reich and H.-P. Loock, "Fabrication and modeling of multimode fiber lenses," *Appl. Opt.* **52**(4), B40–B45 (2013).